Construction of an Ecological Model of Sambucus javanica Blume in China under Different Climate Scenarios Based on Maxent model

Jianfeng Liao
Shenzhen Technology University
Chuqun Yang
Shenzhen Technology University
Qi Shao
Shenzhen Technology University
Qian Sun (sunqian2@sztu.edu.cn)
Shenzhen Technology University
Yulai Han
Shenzhen Technology University

Research Article

Keywords: Sambucus javanica, Traditional Medicinal plants, MaxEnt model, Climate change

Posted Date: November 4th, 2022

DOI: https://doi.org/10.21203/rs.3.rs-2222069/v1

Abstract

Sambucus javanica Blume. is a Chinese native medicinal plant with high medicinal value. In this study, the MaxEnt model was used to explore the relationship between the geographical distribution of S. javanica and environmental factors, and to construct the distribution pattern of S. javanica under different climate scenarios. The results showed that the environmental conditions suitable for the distribution of S. javanica were as follows: precipitation in June ranged from 156.36 mm to 383.25 mm; solar radiation in December ranged from 6750.00 kJ·m-2·day-1 to 10521.00 kJ·m-2·day-1; isothermality ranged from 24.06 to 35.50; precipitation of warmest quarter ranged from 447.92 mm to 825.00 mm. Among them, precipitation and temperature were the key environmental factors affecting the distribution patterns of S. javanica. This plant could grow well mainly in two regions in China, covering a total area of 2.73 × 106 km2. The first region mainly consists of Guizhou, western Hubei, southeastern Chongqing, southwestern Hunan, northern Guangxi, and a small part of eastern Yunnan. The second region mainly consists of Zhejiang, southern Anhui, and northern Fujian. Under the future SSP126 and SSP585 scenarios, potentially suitable habitats in the eastern part of the potential distribution of S. javanica (Jiangxi, Fujian, Zhejiang, and Anhui) might be at risk of habitat fragmentation. Based on the result of this study, Real-time monitoring of wild groups of S. javanica is now recommended to protect its genetic diversity. These findings are supposed to promote the effective conservation and utilization of S. javanica in the future.

1 Introduction

Sambucus javanica Blume, a perennial herb or sub-shrub, is a Chinese native medicinal plant mainly used for acute viral hepatitis, renal edema, rheumatism, traumatic injuries, fractures and other diseases (Bingsheng, 1988; Fang, 2007). And the triterpenes of *S. javanica* has an outstanding anti-hepatitis effect according to modern pharmacological research (Yang et al., 2005; Chen et al., 2020). *S. javanica* also has essential nutrients such as trace elements and amino acids, which can be used in the development of health food (Fang, 2007). The present *S. javanica* is gradually planted large-scale as a traditional Chinese medicinal material with high medicinal value. However, there are no literature reports on the environmental dominant factors and specific suitable distribution of *S. javanica*. In this study, the Maxent model was used to study the suitable distribution area of *S. javanica*, which provides a theoretical basis for large-scale cultivation and resource conservation of *S. javanica*.

As a product of the intersection of computer science and ecology, ecological niche models predict the survival probability of species by calculating the probability of survival based on existing distribution points and geographic layers (Merow et al., 2013). In recent years, with the development of computer science, increasing number of ecological niche models have been developed to meet the needs of ecological research, such as MaxEnt model, DOMAIN model, CLIMEX model, BIOCLIM model, etc (Carpenter et al., 1993; Pattison *et al*., 2008; Liao et al., 2020; Semwal et al., 2021). Maxent model has been widely used in the field of species distribution research because of its advantages of simple operation, good prediction effect and high accuracy (Merow et al., 2013). In addition, the model constructed using the Maxent model can be transferred to different periods or geographic spaces, which can provide a reference for predicting the distribution of suitable habitats in other periods and assessing the risk of species invasion (Kong *et al*.; Zhang et al., 2018; Li et al., 2019).

In this study, the suitable area of *S. javanica* was predicted by Maxent model. Based on the Percent contribution, Permutation importance and Jackknife test, the dominant climatic factors limiting the distribution of *S. javanica* suitable areas were comprehensively evaluated, in order to provide a basis for the scientific development and utilization of *S. javanica*. The potential distributions for three future periods (2040, 2060 and 2080 under SSP126/SSP585) were also predicted and compared with the modern distribution of suitable areas to understand the dominant climatic factors limiting the modern distribution of *S. javanica*.

2. Material And Methods

2.1. Species distribution data

The geographic distribution data of *S. javanica* were extracted from the specimen database and literature data. The herbarium records of *S. javanica* were downloaded from the Chinese Virtual Herbarium (CVH, http://www.cvh.ac.cn/), Plant Photo Bank of China (PPBC, http://ppbc.iplant.cn/), Global Biodiversity Information Facility (GBIF, http://www.gbif.org), National Specimen Information Infrastructure (NSII, http://www.nsii.org.cn/), Plants of the World Online (PWO, http://powo.science.kew.org/), and the Herbarium Kunming Institute of Botany (KUN, http://www.kun.ac.cn/). Additional specific occurrence records were obtained from Flora of China, local flora and other relevant monographs, such as Flora of Jiangxi, Flora of Guizhou, and Flora of Guangxi. In addition, this paper conducted a detailed check, deleting the wrong distribution points and removing the duplicate records. 98 valid geographic distribution points were obtained for further analysis (Fig. 1).

2.2 Download of Environmental variables

The current climate variables were downloaded from the WorldClim Database (version 2.1) (https://www.worldclim.org/). Elevation data were downloaded from Google Earth, and the spatial resolution of the environmental layer was 2.5 min (ca. 4.5 km^2) (Fick and Hijmans, 2017). The SSP126 and SSP585 emission scenarios from the BBC-CSM2-MR Global Climate Models (GCMs) were adopted as the future climate change scenarios (Eyring et al., 2016; O Neill *et al*., 2017; Salawitch et al., 2017). The environmental layers were clipped using ArcMap 10.5 software to convert all layers to ASC format. The altitude and solar radiation variables remain unchanged in the simulation of future potential distributions to maintain the comparability of the model on the spatio-temporal series. The GCS_WGS_1984 projection coordinate system was applied as the map geographic coordinate system.

2.3 Choice of environmental variables

104 environmental variables were considered for model building (Table 1), including temperature (Bio01 ~ 11, Tmin01 ~ 12, Tmax01 ~ 12, Tavg01 ~ 12), precipitation (Bio 12 ~ 19, Prec 01 ~ 12), solar radiation (Srad01 ~ 12), water vapor pressure (Vapr01 ~ 12), wind speed (Wind01 ~ 12) and altitude (Alt). Since

the collinearity among variables will lead to overfitting of the niche model (Graham, 2003), this study applied the Percent contribution and Pearson correlation analysis in order to select variables with a correlation less than 0.8 (Table 2), and to select the one with the largest contribution rate in those with a correlation greater than 0.8 (Qin et al., 2017; Gebrewahid et al., 2020; Liao et al., 2020). As a result, a total of thirteen environmental variables were reserved for model simulation: three temperature variables (Bio 03, Bio 08, Tmin 01), six precipitation variables (Bio 15, Bio 18, Prec 04, Prec 06, Prec 09, Prec 10), and three light variables (Srad 05, Srad06, Srad 12) and one altitude variable (Alt) (Table 2).

Table 1
Environmental variables for modeling

Variable	Description	Variable	Description
Bio 01	Annual Mean Temperature (℃)	Bio 15	Precipitation Seasonality (mm)
Bio 02	Mean Diurnal Range (℃)	Bio 16	Precipitation of Wettest Quarter (mm)
Bio 03	Isothermality	Bio 17	Precipitation of Driest Quarter (mm)
Bio 04	Temperature Seasonality	Bio 18	Precipitation of Warmest Quarter (mm)
Bio 05	Max Temperature of Warmest Month (℃)	Bio 19	Precipitation of Coldest Quarter (mm)
Bio 06	Min Temperature of Coldest Month (℃)	Tmin 01–12	Monthly Average Minimum Temperature of (℃)
Bio 07	Temperature Annual Range (Bio5-Bio6) (℃)	Tmax 01–12	Monthly Average Maximum Temperature (℃)
Bio 08	Mean Temperature of Wettest Quarter (℃)	Tavg 01–12	Monthly Average Temperature (℃)
Bio 09	Mean Temperature of Driest Quarter (℃)	Prec 01–12	Monthly Average Precipitation (mm)
Bio 10	Mean Temperature of Warmest Quarter (℃)	Srad 01–12	Monthly Average Solar Radiation ($kJ \cdot m^{-2} \cdot day^{-1}$)
Bio 11	Mean Temperature of Coldest Quarter (℃)	Wind 01–12	Monthly Average Wind Speed ($m \cdot s^{-1}$)
Bio 12	Annual Precipitation (mm)	Vapr 01–12	Monthly Average Water Vapor Pressure (k·Pa)
Bio 13	Precipitation of Wettest Month (mm)	Alt	Altitude (m)
Bio 14	Precipitation of Driest Month (mm)		

Table 2
Pearson correlation of environmental variables

	Bio03	Bio08	Bio15	Bio18	Prec04	Prec06	Prec09	Prec10	Srad05	Srad06	Srad12	tmin01
Bio08	0.00											
Bio15	0.71	0.12										
Bio18	0.35	0.49	0.47									
Prec04	-0.53	-0.08	-0.70	-0.05								
Prec06	-0.12	0.33	-0.07	0.69	0.57							
Prec09	0.46	0.20	0.42	0.52	-0.38	0.08						
Prec10	0.14	0.16	-0.03	0.20	0.03	0.12	0.46					
Srad05	0.52	0.07	0.34	0.14	-0.58	-0.25	0.48	0.01				
Srad06	-0.07	0.06	-0.09	-0.19	-0.20	-0.27	0.19	-0.07	0.68			
Srad12	0.64	0.07	0.20	0.36	-0.03	0.26	0.40	0.16	0.54	0.08		
tmin01	0.31	0.69	0.20	0.54	0.03	0.49	0.34	0.32	0.05	-0.21	0.50	
Altitude	0.51	-0.67	0.51	-0.08	-0.50	-0.38	0.12	-0.09	0.22	-0.14	0.12	-0.48

2.4 Construction and assessment of MaxEnt model

Geographical distribution points of *S. javanica* were saved as CSV format. The distribution point data and the environmental layer were then imported into the MaxEnt software. 75% of the points were randomly selected for modeling, while 25% of the points were randomly selected for verification, with the maximum number of iterations set to 1000, and repeating the calculation for Bootstrap 10 times (Liao et al., 2020; Yan et al., 2020). According to the probability of species occurrence, the potential distribution of *S. javanica* was divided into the following five grades: unsuitable area (< 0.08), low suitable area (0.08—0.26), generally suitable area (0.26—0.42), moderately suitable area (0.42—0.56), and highly suitable area (> 0.56). The accuracy of the model was evaluated according to the Area under Curve (AUC) under the Receiver Operating Characteristic (ROC) (Jiménez-Valverde, 2012). The importance of variables in the MaxEnt model was assessed through the Jackknife test (Xie et al., 2021). The suitable climatic condition ranges of *S. javanica* were evaluated with the univariate response curve (Graham, 2003; Qin et al., 2017).

3. Results

3.1. Evaluation of Maxent model accuracy

The ROC curve was obtained by simulating the training set through the built-in function of MaxEnt software, and the area under the curve was the AUC value which is generally between 0–1 (Xie et al., 2021). If the AUC value is greater than 0.9, the model prediction effect is excellent, and the closer it comes to 1, the better the model prediction effect is. In this study, the average training AUC was 0.993 while the standard deviation was 0.001. According to the evaluation criteria, the overall prediction accuracy of the model has reached an excellent level, indicating that the model made an accurate prediction on the potential suitable distribution of *S. javanica* (Fig. 2).

3.2 Assessment of environmental variables affecting the distribution of S. javanica

The analysis results of the relative contribution rate of environmental variables in the MaxEnt model were shown in Table 3. Specifically, the percent contribution values of Prec06, Bio18 and Bio03 were 37.90%, 25.50% and 14.00% respectively, and the cumulative value was 77.40%; the permutation importance values of Srad12 and Bio03 were 34.60% and 25.00% respectively, and the cumulative value was 59.60% (Table 3). Among them, precipitation was the most important environmental variables with a cumulative contribution percent of 70.10%, followed by temperature (19.00%), solar radiation (10.00%), and altitude (1.00%). In addition, the jackknife test results of the environmental variables (Fig. 3) indicated that the regularized training gain, test gain and AUC values of Prec06, Bio18 and Srad12 were respectively greater than 2.0, 0.95, and 0.95, which were significantly higher than those of the other environmental variables (see Fig. 3). Among them, the environmental variable with the highest gain is Prec06, which indicated that this environmental variable contained the most useful information on the distribution of *S. javanica*. When Bio03 or Srad12 was ignored to build the model, the regularized training gain was obviously decreased, showing that these two environmental variables contained a lot of information not found in the rest of the variables (Fig. 3). In summary, Prec06, Bio18, Bio03, and Srad12 were the key environmental limiting factors that significantly influence the distribution of *S. javanica*.

Table 3
Relative contribution rate of environmental variables

Variable	Percent contribution (%)	Permutation importance (%)
Prec06	37.90	0.50
Bio18	25.50	0.90
Bio03	14.00	25.00
Srad12	6.60	34.60
Tmin01	4.90	11.40
Prec04	3.10	1.60
Srad05	2.90	13.10
Bio15	2.50	0.90
Alt	1.00	1.60
Prec09	0.60	0.90
Srad06	0.50	6.90
Prec10	0.50	0.70
Bio08	0.10	1.90

3.3 Assessment of the optimum environmental conditions

In order to conduct a further analysis of the influence of the environmental variables on the distribution of *S. javanica*, the 4 main environmental variables Prec06, Bio18, Bio03, and Srad12 were imported into MaxEnt models respectively. A univariate model was established to fit the univariate response curve, which shows the relationship between the main environmental variables and the geographical distribution probability of *S. javanica* (Fig. 4). When the existence probability was greater than 50%, the corresponding environmental factor value was suitable for the growth of the species (Awade et al., 2012). According to the univariate response curve of environmental factors, the optimum environmental conditions for the growth and distribution of *S. javanica* were as follows: precipitation in June ranged from 156.36 mm to 383.25 mm; precipitation of warmest quarter ranged from 447.92 mm to 825.00 mm; isothermality ranged from 24.06 to 35.50; solar radiation in December ranged from 6750.00 $kJ \cdot m^{-2} \cdot day^{-1}$ to 10521 $kJ \cdot m^{-2} \cdot day^{-1}$ (Fig. 4).

3.4 Prediction of distribution pattern under current climate condition

The results indicated that the suitable regions of *S. javanica* were widely distributed in southern China (Table 4 and Fig. 5a). From the perspective of administrative division, *S. javanica* is suitable for growing in 25 provinces and cities (Table 4). Among them, Guizhou was the most suitable area, followed by Zhejiang, Hunan, Chongqing, Fujian, Guangxi, Hubei, Jiangxi, Anhui, Guangdong, Shaanxi and eastern fringe of Yunnan. The current potential suitable areas of *S. javanica* in China were 2.73×10^6 km^2, and among them the highly suitable areas were 6.63×10^5 km^2 (24.27%); the moderately suitable areas were 7.93×10^5 km^2 (29.04%); the generally suitable areas were 6.86×10^5 km^2 (25.11%); the low suitable areas were 5.89×10^5 km^2 (21.58%). According to the current

suitable distribution map of *S. javanica* (Fig. 5a), *S. javanica* is mainly suitable for growing in two regions in China. The first region, which was also the most important region (as shown in the blue oval in Fig. 5a), mainly consists of Guizhou, western Hubei, southeastern Chongqing, southwestern Hunan, northern Guangxi and a small part of eastern Yunnan, covering a cumulative high suitable distribution area of 4.38×10^5 km^2 (66.16% of the total high suitable areas). The second region mainly consists of Zhejiang, southern Anhui and northern Fujian, covering a cumulative high suitable distribution area of 1.24×10^5 km^2 (18.67% of the total high suitable areas) (as shown in the black oval in Fig. 5a).

Table 4
The modern suitable distribution areas of *S. javanica* in various administrative regions.

Provinces or cities	Total areas (km^2)	Highly suitable areas		Moderately suitable areas		Generally suitable areas		Low suitable areas		Total suita
		Area (km^2)	Percentage (%)	Area (km^2)	Percentage (%)	Area (km^2)	Percentage (%)	Area (km^2)	Percentage (%)	Area (km^2)
Guizhou	159307.69	141857.15	89.05	17242.59	10.82	207.95	0.13	\	\	159307.69
Zhejiang	92486.15	56631.95	61.23	28489.27	30.80	7364.93	7.96	\	\	92486.15
Hunan	193532.95	95553.43	49.37	96818.46	50.03	1161.06	0.60	\	\	193532.95
Chongqing	77219.10	32405.68	41.97	43132.48	55.86	1680.94	2.18	\	\	77219.10
Fujian	108983.59	44900.06	41.20	42629.93	39.12	15128.43	13.88	6325.17	5.80	108983.59
Guangxi	209129.26	82816.43	39.60	62679.86	29.97	63528.99	30.38	103.98	0.05	209129.26
Hubei	175285.25	53893.93	30.75	61588.12	35.14	59803.20	34.12	\	\	175285.25
Jiangxi	152427.99	46286.40	30.37	91671.68	60.14	14469.91	9.49	\	\	152427.99
Anhui	133383.16	22354.72	16.76	35316.99	26.48	29165.11	21.87	33064.19	24.79	119901.01
Guangdong	154784.76	17883.77	11.55	61137.56	39.50	72176.28	46.63	3587.15	2.32	154784.76
Shaanxi	203445.28	23186.52	11.40	53841.95	26.47	16740.05	8.23	30603.44	15.04	124371.96
Yunnan	342183.16	31955.12	9.34	71379.14	20.86	93352.61	27.28	138945.84	40.61	335632.71
Sichuan	454511.29	11038.73	2.43	92122.24	20.27	138893.85	30.56	143434.11	31.56	385488.93
Henan	160988.63	1663.61	1.03	15249.73	9.47	53027.47	32.94	39424.02	24.49	109364.83
Taiwan	31643.18	311.93	0.99	4245.66	13.42	10640.15	33.63	14036.68	44.36	29234.42
Tibet	1141113.08	51.99	0.00	9860.34	0.86	34779.78	3.05	54465.80	4.77	99157.91
Gansu	414532.73	17.33	0.00	2720.69	0.66	19945.95	4.81	63477.00	15.31	86160.97
Jiangsu	97199.70	\	\	2408.76	2.48	49267.03	50.69	23463.79	24.14	75139.58
Hainan	29061.13	\	\	\	\	\	\	21141.67	72.75	21141.67
Qinghai	712093.1	\	\	\	\	\	\	7642.19	1.07	7642.19
Shanxi	159273.04	\	\	\	\	86.65	0.05	7087.66	4.45	7174.31
Shanghai	4817.53	\	\	485.22	10.07	4332.31	89.93	\	\	4817.53
Shandong	153450.42	\	\	\	\	\	\	1472.99	0.96	1472.99
Ningxia	52576.91	\	\	\	\	\	\	953.11	1.81	953.11
Statistical	5413429.08	662739.43	24.27	793020.67	29.04	685752.65	25.11	589228.79	21.58	2730810.8

Note: "\" indicates that there is no corresponding suitable distribution in this region. Black arrows indicate the table is sorted according to the percentage of h area

3.5 Prediction of future distribution under climate changes

The potential suitable regions of *S. javanica* in the 2040s, 2060s, 2080s, and 2100s were constructed under the SSP126 and SSP585 scenarios (Fig. 5b-5i). Under the climate scenario SSP126, the total suitable areas in the 2040s, 2060s, 2080s and 2100s were 2.60×10^6 km^2, 2.66×10^6 km^2, 2.60×10^6 km^2, and 2.57×10^6 km^2 respectively (Fig. 6). Compared with the modern condition, the distribution area of *S. javanica* decreased obviously by the 2040s (reduced by 1.38×10^5 km^2 relative to the current distribution), and recovered slightly by the 2060s (recovered by 6.07×10^4 km^2 relative to that by the 2040s), and then gradually decreased by the 2080s and 2100s (reduced by 55.87×10^4 km^2 and 8.87×10^4 km^2, respectively, relative to that by the 2060s) (Fig. 6). Under the climate scenario SSP585, the suitable total areas for 2040s, 2060s, 2080s and 2100s are 2.67×10^6 km^2, 2.66×10^6 km^2, 2.68×10^6 km^2 and 2.74×10^6 km^2, respectively. Compared with the modern condition, by the 2040s and 2060s, the suitable distribution area of *S. javanica* obviously decreased (reduced by 7.73×10^4 km^2 relative to the current distribution), and gradually recovered by the 2080s (recovered by 7.37×10^4 km^2 relative to that by the 2060s), and then small expanded by the 2100s (increased by 5077 km^2 relative to the current distribution) (Fig. 6).

In general, in contrast to the climate scenario SSP126, the impact on the suitable distribution area of *S. javanica* for SSP585 was relatively minor. The distribution areas of *S. javanica* displayed an overall decreasing trend under the SSP126 scenario. However, under the SSP585 scenario, although the distribution area of *S. javanica* was reduced relative to the current distribution by the 2040s and 2060s, the distribution area was steadily recovered by the 2080s and even gradually increases by the 2100s.

4 Discussion

4.1 Response of suitable distribution to environmental variables

It is of great significance for ecological management to explore the changes in the geographical distribution of species caused by climate change (Hamann and Wang, 2006; Paź-Dyderska et al., 2021; Varol et al., 2021). O Neill and Kriegler *et al* (2017) predicted that the average global temperature would be more than 4 ℃ above pre-industrial levels by 2100s, which would alter the geographic distribution of many species (Lenoir et al., 2008; Bellard et al., 2012; Hundessa et al., 2018; Bouahmed et al., 2019). The profound impact on the distribution change of species might alter the function and structure of terrestrial ecosystems in turn (Huang et al., 2021). Therefore, assessing the impact of climate change on the spatial distribution of different species will help address issues related to changes in the distribution and range of various species.

This study predicted the potential distribution pattern of *S. javanica* under current and future climatic conditions in China using the MaxEnt model. From the phytogeographic point of view, *S. javanica* was mainly located in the subtropical region of China (south of the Qinling Mountains-Huaihe River Line and east of the Hengduan Mountains). The presence of mountain ranges affected the distribution of plants and animals (Elsen et al., 2018; Odland, 2010). In this study, the Qinling-Huaihe line was found to be the northern boundary of *S. javanica* distribution, and the western boundary of *S. javanica* was the Hengduan Mountains. The Qinling Mountains-Huaihe River Line serves as the dividing line between the southern and northern regions of China, with significant differences in geography, climate and environment (González-Prieto *et al*., 2016). The south region of the line has a humid, warm and rainy climate, with an average January temperature above 0°C and average annual precipitation above 800mm (Li et al., 2018). This boundary is also the dividing line between the subtropical monsoon and temperate monsoon climates, and is considered to be the main parameter affecting the distribution of many species (Zhou et al., 2011; Pan et al., 2020; Xie et al., 2021). Moreover, the warm and humid airflow from the Indian Ocean is blocked by two tall east-west mountain ranges (the Himalaya and the Gondola) and enters China along the north-south Hengduan mountain range, bringing abundant rain to the Tibetan Plateau (Li et al., 2018; Kramer et al., 2010; Xu et al., 2019). Therefore, the Qinling-Huaihe line and the Hengduan Mountains are the boundaries of the 800 mm equivalent precipitation area in China, which overlap with the modern distribution boundary of *S. javanica* (Fig. 5a). The cumulative contribution of two precipitation factors (Prec01 and Bio18) with a value of 63.4% (Table 3) was also further evidence that precipitation was critical to the distribution of *S. javanica*. This result suggested that the limiting effect of precipitation on the growth of *S. javanica* might be one of the main reasons why its modern distribution is mainly concentrated in the subtropical region of South China.

In addition, the altitude-induced temperature change (decrease about 6℃ per 1000 meter elevation) was also an important factor affecting the distribution of plants (Rangwala & Miller, 2012). The Yunnan-Guizhou Plateau, bounded by the Wumeng Mountains, was divided into the Yunnan Plateau (altitude 3000–4000 m) and the Guizhou Plateau (altitude 2000–2400 m) (Zheng et al., 2020). In summer, the temperature of the Yunnan-Guizhou Plateau was lower than that of the same latitude region due to its higher altitude. In winter, the temperature of Yunnan-Guizhou Plateau was higher than that of the same latitude region due to the plateau is at the intersection of the Pacific and Indian Ocean monsoons (Yang, 2008). The unique geographical location of the Yunnan-Guizhou Plateau results in low temperatures in summer and high temperatures in winter, also leading to its annual temperature difference smaller than that of the same geographical latitude (Yang, 2008).

This might be the main reason why the Yunnan plateau has adequate precipitation (1000–1200 mm per year), but the distribution suitability class of *S. javanica* in the region is largely low suitability distribution area.

4.2 Changes of suitable habitat in future climate scenarios

Research into the impact of future climate changes on plants could be beneficial to develop strategies towards the challenges caused by climate change (Liao et al., 2020). The sixth iteration of the Climate Model Intercomparison Project (CMIP6) is widely applied to discuss the impact of future climate change on global ecology and economic development (Xu et al., 2022; Tan et al., 2022). The CMIP6 modeled future climatic conditions by combining possible future socio-economic conditions (Shared Socio-economic Pathways) and different greenhouse gas (GHG) emission scenarios (Representative Concentration Pathways, RCPs) (O'Neill et al., 2016). In this study, the climate scenarios SSP126 and SSP585 were used as a background to simulate the future distribution of *S. javanica*. The SSP126 scenario represented a sustainable development path. In this scenario, fossil energy dependence and global carbon dioxide emissions would be greatly reduced, and the radiative forcing level would approach $2.6Wm^{-2}$. Carbon dioxide emissions are expected to be reduced to zero by around 2050s, and the global temperature would be about 1.8°C higher than today by around 2100s (O'Neill et al., 2016). The SSP585 scenario represented the traditional path of economic development. In this scenario, people solve social and economic problems by emphasizing self-interest and rapid development. The radiative forcing level would approach $5.8Wm^{-2}$. Carbon dioxide emissions are expected to double relative to current levels by around 2050s, and the global temperature would be about 4.4°C higher than today by around 2100s (O'Neill et al., 2016).

In this study, the variation of the suitable distribution area of *S. javanica* are investigated under two different environmental strategies. The results showed that the suitable distribution area of *S. javanica*, under the SSP126 climate scenario, exhibited a shrinking trend relative to the current suitable distribution area. However, under the SSP126-2080s scenario, the highly suitable distribution area of *S. javanica* showed a significant increase, caused by the conversion of low, generally and moderately suitable distribution areas to highly suitable distribution areas. This suggested that there could be a risk of *S. javanica* suitable habitats loss and fragmentation under the SSP126 climate scenario. Although the suitable distribution area of *S. javanica* showed a shrinking trend under the SSP585-2040s and SSP585-2060s, the distribution was gradually recovered and became stable after the SSP585-2080s. Meanwhile, in the context of future

global warming, the low suitability distribution of *S. javanica* in the Yunnan Plateau showed a trend of conversion to moderate suitability distribution, probably caused by the relatively low temperature at high altitudes that provided a potential geographic barrier for *S. javanica* against future climate warming (Xie et al., 2021). Summary, although the distribution areas of *S. javanica* might be affected to some extent under future climate scenarios due to increased precipitation and temperature, the overall distribution pattern of *S. javanica* was unlikely to change. This suggested that *S. javanica* could cope with the effects of future global warming on its distribution pattern.

4.3 Prospects and Suggestions

The active substances (mostly secondary metabolites) produced by medicinal plants serve as direct indicators for judging its quality. Previous researches showed that the contents, types and proportions of active substances are strongly related to environmental factors such as illumination, moisture and temperature (Penuelas & Llusia, 1997; Liu et al., 2016). However, a suitable growth environment does not necessarily lead to the accumulation of more active ingredients in the medicinal plants. They might also produce more active substances in response to environmental stress under unfavorable growth conditions (Wang et al. 2016; Alhaithloul *et al*., 2020; Toivonen et al., 1992; Jochum et al. 2007). For example, the contents of myricetin-3-O-rhamnoside in the roots of *Limonium bicolor* (Bag.) Kuntze were significantly increased under salt stress (Wang et al. 2016). In the medicinal plants *Mentha piperita* and *Catharanthus roseus*, the levels of tannins, terpenoids and alkaloids were significantly increased under the combined heat/drought stress (Alhaithloul *et al*., 2020). At present, the relationship between the environmental factors and the active ingredients of *S. javanica* is currently not clear. Therefore, the influence of environmental factors on the medicinal active ingredients of *S. javanica* is a major research focus for the future.

5 Conclusion

This research indicated that *S. javanica* were mainly distributed in 25 provinces and cities in China (subtropical regions of China). Among them, Guizhou, Zhejiang, Hunan, Chongqing, Fujian, Hubei and Jiangxi were the most suitable regions for *S. javanica* introduction and cultivation (highly suitable areas > 30%). Precipitation in June (Prec06), precipitation of warmest quarter (Bio18), isothermality (Bio03) and average solar radiation in December (Srad12) were mainly climatic factors that limit the distribution of *S. javanica*. Furthermore, future climate changes might have little impact on the distribution patterns of *S. javanica*. As a traditional Chinese herbal medicine, *S. javanica* has a rich variety of active ingredients (mainly including flavonoids, triterpenoids, steroidals, volatile oils, and phenylpropanioids), our study provides a theoretical basis for the exploitation of *S. javanica*, but further studies on the effects of environmental factors on the active ingredients of *S. javanica* are needed in order to produce high-quality *S. javanica* raw materials.

Declarations

Competing Interests Statement

All authors declare that No conflict of interest exists.

Author Contributions: Qian Sun: Conceptualization, writing—review and editing, supervision, visualization, project administration, funding acquisition; Yulai Han: Conceptualization, resources, writing—review and editing, supervision, project administration, funding acquisition; Jianfeng Liao: Conceptualization, writing—original draft preparation, writing—review and editing, visualization; Chuqun Yang: investigation, writing—review and editing; Qi Shao: investigation, writing—review and editing. All authors have read and agreed to the published version of the manuscript.

Funding: This work was supported by the Natural Science Foundation of Top Talent of SZTU [Grant no. 2019010801010, 2019010801009]

References

1. Awade, M., Boscolo, D. & Metzger, J.P., (2012). Using binary and probabilistic habitat availability indices derived from graph theory to model bird occurrence in fragmented forests. *Landscape Ecology*, 27 (02), p. 185-198. doi:10.1007/s10980-011-9667-2
2. Alhaithloul, H. A., Soliman, M. H., Ameta, K. L., El-Esawi, M. A. & Elkelish, A., (2019). Changes in ecophysiology, osmolytes, and secondary metabolites of the medicinal plants of *Mentha piperita* and *Catharanthus roseus* subjected to drought and heat stress. *Biomolecules*, 10 (1), p. 43. doi:10.3390/biom10010043
3. Bingsheng, X., (1988). *Flora of China*, Volume 72: Caprifoliaceae. Bejing China: China social sciences press.
4. Bellard, C., Bertelsmeier, C., Leadley, P., Thuiller, W. & Courchamp, F., (2012). Impacts of climate change on the future of biodiversity. *Ecology Lett*ers, 15, p. 365-377. doi: 10.1111/j.1461-0248.2011.01736.x
5. Bouahmed, A., Vessella, F., Schirone, B., Krouchi, F. & Derridj, A., (2019). Modeling *Cedrus atlantica* potential distribution in North Africa across time: new putative glacial refugia and future range shifts under climate change. *Regional Environmental Change*, 19 (06), p. 1667-1682. doi:10.1007/s10113-019-01503-w
6. Carpenter, G., Gillison, A.N. & Winter, J., (1993). DOMAIN: a flexible modelling procedure for mapping potential distributions of plants and animals. *Biodivers Conserv*, 2, p. 667-680. doi: 10.1007/bf00051966
7. Chen, F., Liu, D., Wang, W., Lv, X., Li, W., Shao, L. & Wang, W., (2020). Bioactive triterpenoids from *Sambucus javanica* Blume. *Natural Product Research*, 34 (19), p. 2816-2821. doi: 10.1080/14786419.2019.1596092
8. Eyring, V., Bony, S., Meehl, G.A., Senior, C.A., Stevens, B., Stouffer, R.J. & Taylor, K.E., (2016). Overview of the Coupled Model Intercomparison Project Phase 6 (CMIP6) experimental design and organization. *Geoscientific Model Development*, 9 (05), P. 1937-1958. doi:10.5194/gmd-9-1937-2016
9. Elsen, P. R., W.B. Monahan and A.M. Merenlender, (2018). Global patterns of protection of elevational gradients in mountain ranges. *Proceedings of the National Academy of Sciences*, 115 (23), p. 6004-6009. doi:10.1073/pnas.1720141115

10. Fang, J., (2007). Exploitation and utilization of *Sambucus chinensis*. *Forest By Product and Speciality in China*, (06), p. 85-87. doi: 10.3969/j.issn.1001-6902.2007.06.035
11. Fick, S.E. & Hijmans, R.J., (2017). WorldClim 2: new 1-km spatial resolution climate surfaces for global land areas. *International Journal of Climatology*, 37 (12), P. 4302-4315. doi:10.1002/joc.5086
12. Graham, M.H., (2003). Confronting multicollinearity in ecological multiple regrssion. *Ecology*, 84 (11), p. 2809-2815. doi:10.1890/02-3114González-Prieto, A., Bayly, N., Colorado Z., G. & Hobson, K., (2016). Topography of the Andes Mountains shapes the wintering distribution of a migratory bird. *Diversity and Distributions*. 23 (02), p. 01-12. doi: 10.1111/ddi.12515
13. Gebrewahid, Y., Abrehe, S., Meresa, E., Eyasu, G., Abay, K., Gebreab, G., Kidanemariam, K., Adissu, G., Abreha, G. & Darcha, G., (2020). Current and future predicting potential areas of *Oxytenanthera abyssinica* (A. Richard) using MaxEnt model under climate change in Northern Ethiopia. *Ecological Processes*., 9 (01), P. 1-15. doi:10.1186/s13717-019-0210-8
14. Hamann, A., Wang, T., (2006). Potential effects of climate change on ecosystem and tree species distribution in British Columbia. *Ecology*, 87 (11), p. 2773-2786. doi:10.1890/0012-9658(2006)87[2773:PEOCCO]2.0.CO;2
15. Hundessa, S., Li, S., Liu, D.L., Guo, J., Guo, Y., Zhang, W. & Williams, G., (2018). Projecting environmental suitable areas for malaria transmission in China under climate change scenarios. *Environmental Research*, 162, p. 203-210. doi.:10.1016/j.envres.2017.12.021
16. Huang, R., Yu, T., Zhao, H., Zhang, S., Jing, Y. & Li, J., (2021). Prediction of suitable distribution area of the endangered plant *Acer catalpifolium* under the background of climate change in China. J. *Journal of Beijing Forestry University*, 43 (05), p. 33–43. doi:10.12171/j.1000-1522.20200254
17. Jochum, G.M., Mudge, K.W. & Thomas, R.B., (2007). Elevated temperatures increase leaf senescence and root secondary metabolite concentrations in the understory herb *Panax quinquefolius* (Araliaceae). *American Journal of Botany*, 94(5), p. 819-826. doi: 10.3732/ajb.94.5.819.
18. Jiménez-Valverde, A., (2012). Insights into the area under the receiver operating characteristic curve (AUC) as a discrimination measure in species distribution modelling. *Global Ecology and Biogeography*, 21 (04), p. 498-507. doi:10.1111/j.1466-8238.2011.00683.x
19. Kramer, A., Herzschuh, U., Mischke, S. & Zhang, C., (2010). Holocene treeline shifts and monsoon variability in the Hengduan Mountains (southeastern Tibetan Plateau), implications from palynological investigations. *Palaeogeography, Palaeoclimatology, Palaeoecology*, 286 (01), p. 23-41. doi:10.1016/j.palaeo.2009.12.001.
20. Kong, F., Tang, L., He, H., Yang, F., Tao, J., Wang, W., (2021) Assessing the impact of climate change on the distribution of Osmanthus fragrans using Maxent. *Environ Sci Pollut R*, p. 1-9. doi: 10.1007/s11356-021-13121-3
21. Lenoir, J., Gégout, J.C., Marquet, P. A., De Ruffray, P. & Brisse, H., (2008). A significant upward shift in plant species optimum elevation during the 20th century. *Science*, 320 (5884), p. 1768-1771. doi:10.1126/science.1156831
22. Liu, W., Yin, D., Li, N., Hou, X., Wang, D., Li, D. & Liu, J. (2016). Influence of environmental factors on the active substance production and antioxidant activity in *Potentilla fruticos*a L. and its quality assessment. *Scientific Reports*, 6 (1), P. 28591. doi:10.1038/srep28591
23. Li, S., Lu, J., Yan, J., Liu, X., Kong, F. & Wang, J., (2018). Spatiotemporal variability of temperature in northern and southern Qinling Mountains and its influence on climatic boundary. *Acta Geographica Sinica*, 73 (01), p. 13-24. doi: 10.11821/dlxb201801002
24. Li, W., Shi, M., Huang, Y., Chen, K., Sun, H., Chen, J., (2019). Climatic Change Can Influence Species Diversity Patterns and Potential Habitats of Salicaceae Plants in China. *Forests*, 10 (3), p. 220. doi: 10.3390/f10030220
25. Liao, J.F., Yi Z.L., Li S.C. & Xiao L., (2020). Maxent modeling for predicting the potentially geographical distribution of *Miscanthus nudipes* under different climate conditions. *Acta. Ecologica. Sinica*., 40 (20), P. 8297-8305. doi:10.5846/stxb201911092361
26. Merow, C., Smith, M.J. & Silander Jr, J.A., (2013). A practical guide to MaxEnt for modeling species' distributions: what it does, and why inputs and settings matter, *Ecography*, 36(10), p. 1058-1069. doi: 10.1111/j.1600-0587.2013.07872.x
27. Odland, A., (2010). Importance of mountain height and latitude for the altitudinal distribution limits of vascular plants in Scandinavia: Are the mountains high enough? *Fennia*, 188 (02), p. 149-162. http://www.helsinki.fi/maantiede/geofi/fennia/
28. O'Neill, B.C., Tebaldi, C., van Vuuren, D., Eyring, V., Friedlingstein, P., Hurtt, G., Knutti, R., Kriegler, E., Lamarque, J., Lowe, J., Meehl, J., Moss, R., Riahi, K. & Sanderson, B.M. (2016). The Scenario Model Intercomparison Project (ScenarioMIP) for CMIP6. *Geoscientific Model Development*, 9 (09), p. 3461–3482. doi: 10.5194/gmd-9-3461-2016
29. O'Neill, B.C., Kriegler, E., Ebi, K.L., Kemp-Benedict, E., Riahi, K., Rothman, D.S., van Ruijven, B.J., van Vuuren, D.P., Birkmann, J., Kok, K., Levy, M. & Solecki, W., (2017). The roads ahead: Narratives for shared socioeconomic pathways describing world futures in the 21st century. *Global Environmental Change*, 42, p. 169-180. doi: 10.1016/j.gloenvcha.2015.01.004
30. Penuelas, J. & Llusia, J. (1997). Effects of carbon dioxide, water supply, and seasonality on terpene content and emission by *Rosmarinus officinalis*. *Journal of Chemical Ecology*, 23 (4), p.979-993. doi: 10.1023/B:JOEC.0000006383.29650.d7
31. Pattison, RR., Mack, RN., (2008). Potential distribution of the invasive tree Triadica sebifera (Euphorbiaceae) in the United States: evaluating CLIMEX predictions with field trials. *Glob Change Biol,*14(4), p. 813-826. doi: 10.1111/j.1365-2486.2007.01528.x
32. Pan, J., X Fan, Luo, S., Zhang, Y. & Qian, Z., (2020). Predicting the potential distribution of two varieties of litsea coreana (leopard-skin camphor) in china under climate change. *Forests*, 11 (11), p. 1159. doi: 10.3390/f11111159
33. Paź-Dyderska, S., Jagodziński, A.M. & Dyderski, M.K., (2021). Possible changes in spatial distribution of walnut (*Juglans regia* L.) in Europe under warming climate. *Regional Environmental Change*, 21 (01). doi:10.1007/s10113-020-01745-z
34. Qin, A., Liu, B., Guo, Q., Bussmann, R.W., Ma, F., Jian, Z., Xu, G. & Pei, S., (2017). Maxent modeling for predicting impacts of climate change on the potential distribution of *Thuja sutchuenensis* Franch., an extremely endangered conifer from southwestern China. *Global Ecology and Conservation*, 10, P. 139-146. doi: 10.1016/j.gecco.2017.02.004

35. Rangwala, I. & Miller, J. R. (2012). Climate change in mountains: A review of elevation-dependent warming and its possible causes. *Climatic Change*, 114 (3-4), p. 527-547. doi: /s10584-012-0419-3

36. Salawitch, R., Bennett, B., Hope, A., Tribett, W. & Canty, T., (2017). *Earth's Climate System*. IN: Dodson, J., ed. *Paris Climate Agreement: Beacon of Hope*. Springer Open, Cham. p. 1-42. https://link.springer.com/content/pdf/10.1007/978-3-319-46939-3.pdf

37. Semwal, D.P., Pandey, A., Gore, P.G., Ahlawat, S.P., Yadav, S.K., Kumar, A., (2021). Habitat prediction mapping using BioClim model for prioritizing germplasm collection and conservation of an aquatic cash crop 'makhana' (Euryale ferox Salisb.) in India. *Genet Resour Crop Ev*, 68, p. 3445-3456. doi: 10.1007/s10722-021-01265-7

38. Toivonen, L., Laakso, S. & Rosenqvist, H., (1992). The effect of temperature on growth, indole alkaloid accumulation and lipid composition of *Catharanthus roseus* cell suspension cultures. *Plant Cell Reports,* 11, p. 390-394. doi: 10.1007/BF00234367

39. Tan, L., Feng, P., Li, B., Huang, F., Liu, D. L., Ren, P., Liu, H., Srinivasan, R. & Chen, Y. (2022). Climate change impacts on crop water productivity and net groundwater use under a double-cropping system with intensive irrigation in the haihe river basin, china. *Agricultural Water Management*, 266. doi: 10.1016/j.agwat.2022.107560

40. Varol, T., Canturk, U., Cetin, M., Ozel, H.B. & Sevik, H., (2021). Impacts of climate change scenarios on European ash tree (*Fraxinus excelsior* L.) in Turkey. *Forest Ecology and Management.* 491, p. 119199. doi: 10.1016/j.foreco.2021.119199

41. Wang, L., Li, W., Ma, L., Chen, J., Lü, H. & Jian, T. (2016). Salt stress changes chemical composition in limonium bicolor (bag.) kuntze, a medicinal halophytic plant. *Industrial Crops and Products*, 84, p. 248-253. doi: 10.1016/j.indcrop.2016.01.050

42. Xu, J., Koldunov, N.V., Remedio, A.R.C., Sein, D.V., Rechid, D., Zhi, X., Jiang, X., Xu, M., Zhu, X., Fraedrich, K. & Jacob, D., (2019). Downstream effect of Hengduan Mountains on East China in the REMO regional climate model. *Theoretical and Applied Climatology*, 135 (03), p. 1641-1658. doi: 10.1007/s00704-018-2721-0

43. Xie, C., Huang, B., Jim, C.Y., Han, W. & Liu, D., (2021). Predicting differential habitat suitability of *Rhodomyrtus tomentosa* under current and future climate scenarios in China. *Forest Ecology and Management*. 501, p. 119696. doi: 10.1016/j.foreco.2021.119696

44. Xu, S., Liu, De., Li, T., Fu, Q., Liu, Do., Hou, R., Meng, F., Li, M. & Li, Q., (2022). Spatiotemporal evolution of the maximum freezing depth of seasonally frozen ground and permafrost continuity in historical and future periods in heilongjiang province, china. *Atmospheric Research*, 274. doi:10.1016/j.atmosres.2022.106195

45. Yang, W., Wang, X., Wang, M., Xu, Y., Lu, D. & Liu, C., (2005). Protective effects of the granule of Sambucus chinensis lindl on acute hepatic injury. *Journal of Chinese Medicinal Materials*. 28 (12), p. 1085-1089. doi: 10.3969/j.issn.1673-7555.2007.22.005

46. Yang R.H. (2008). Current Situation and Utilization Research of Wild Woody Vine Resources in Guizhou. *Seed*, 27 (1), p. 55-57. doi: 10.3969/j.issn.1001-4705.2008.01.016

47. Yan, H., Feng, L., Zhao, Y., Feng, L., Wu, D. & Zhu, C., (2020). Prediction of the spatial distribution of *Alternanthera philoxeroides* in China based on ArcGIS and MaxEnt. *Global Ecology and Conservation.* 21, p. e00856. doi: 10.1016/j.gecco.2019.e00856

48. Zhou, Q., Bian, J. & Zheng, J., (2011). Variation of air temperature and thermal resources in the Northern and Southern regions of the Qinling Mountains from 1951 to 2009. *Acta Geographica Sinica*, 66 (09), p. 1211-1218. doi: 10.1007/s11589-011-0776-4

49. Zhang, K., Yao, L., Meng, J., Tao, J., (2018). Maxent modeling for predicting the potential geographical distribution of two peony species under climate change. *Sci Total Environ*, 634, p. 1326-1334. doi: doi:10.1016/j.scitotenv.2018.04.112

50. Zheng, T., He, X., Ye, H., Fu, W., Peng, M. & Gou, G. (2020). Phylogeography of the rare and endangered lycophyte. *Isoetes yunguiensis*. *PeerJ*, 8, p. e8270-e8270. doi: 10.7717/peerj.8270

Figures

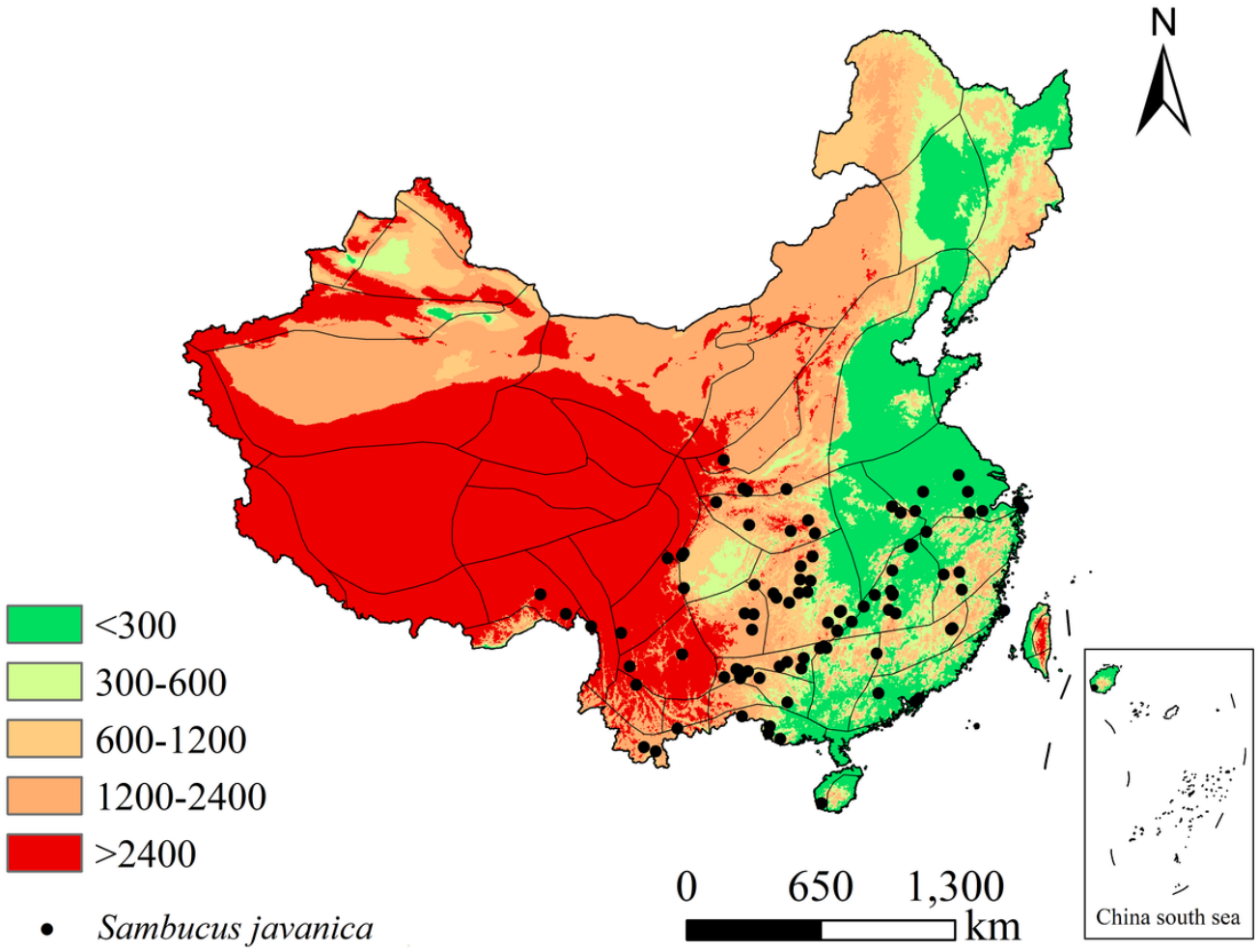

Figure 1

The distribution points of *S. javanica* in administrative division of China with reference to altitude.

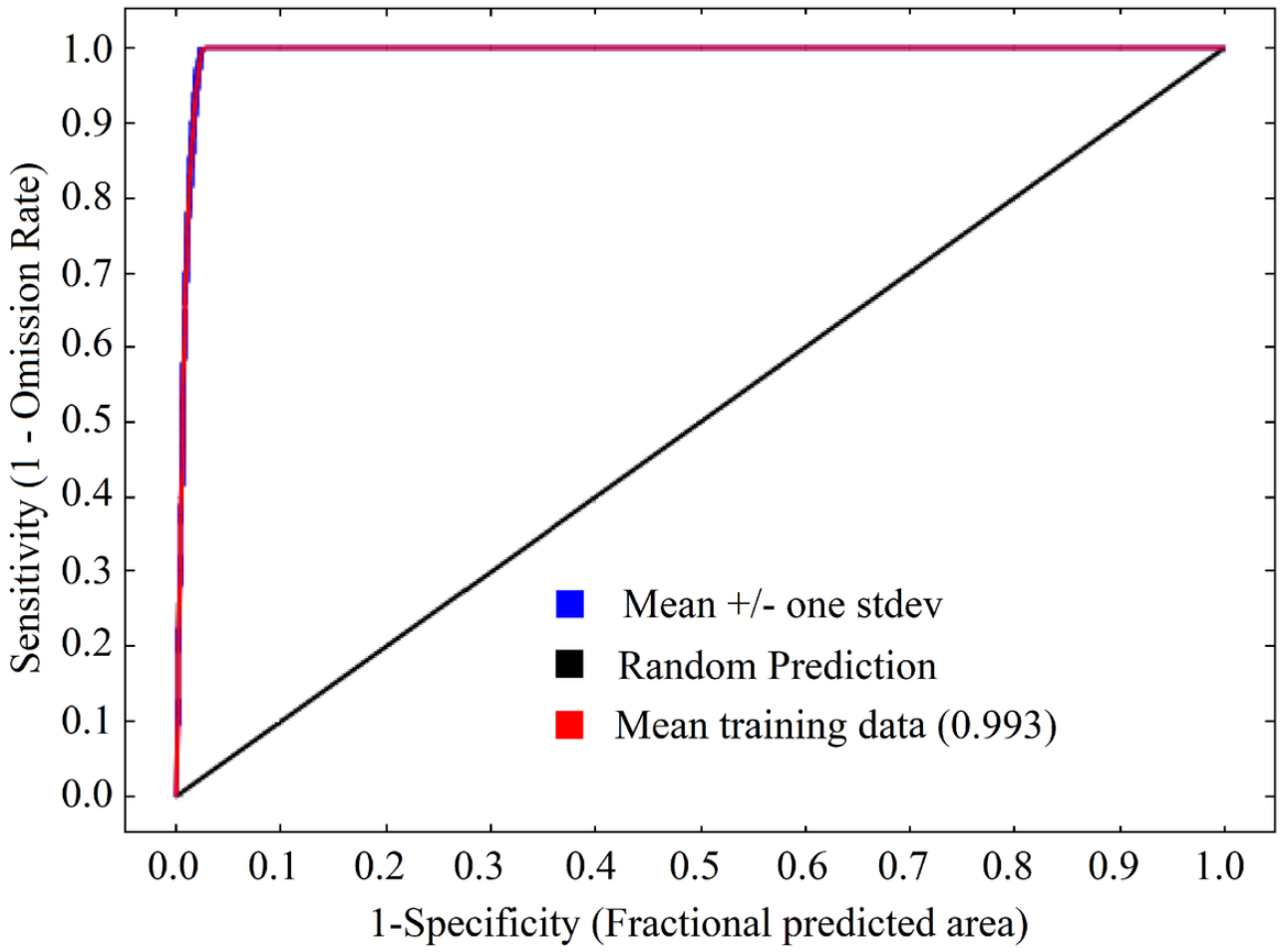

Figure 2

ROC curve verification of the distribution of *S. javanica* predicted by MaxEnt model (10 replicated runs).

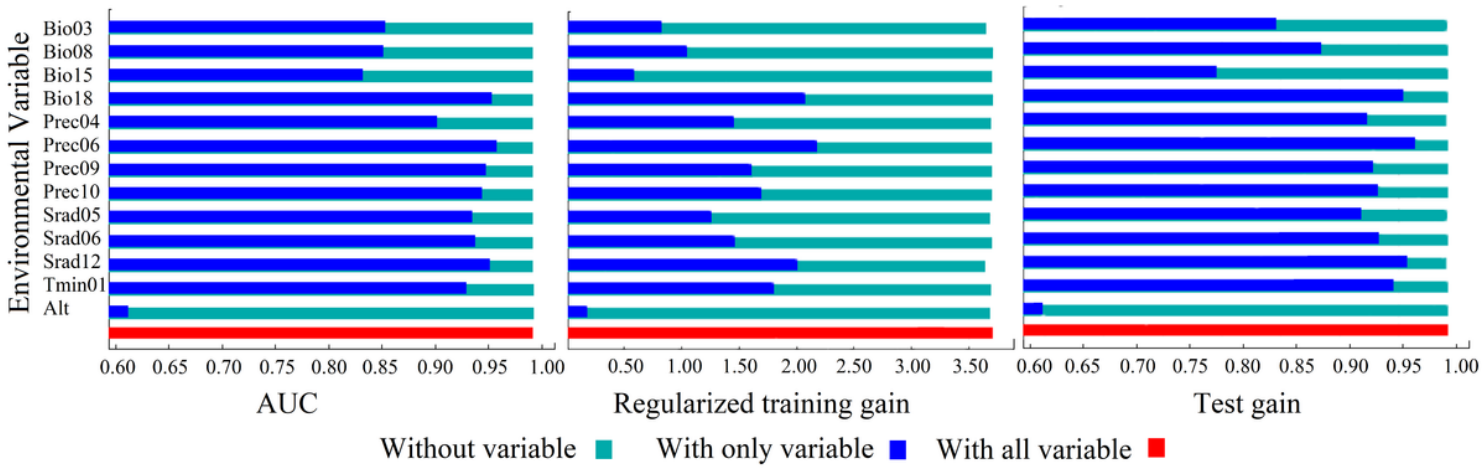

Figure 3

Jackknife test of the importance of environmental variables in MaxEnt model.

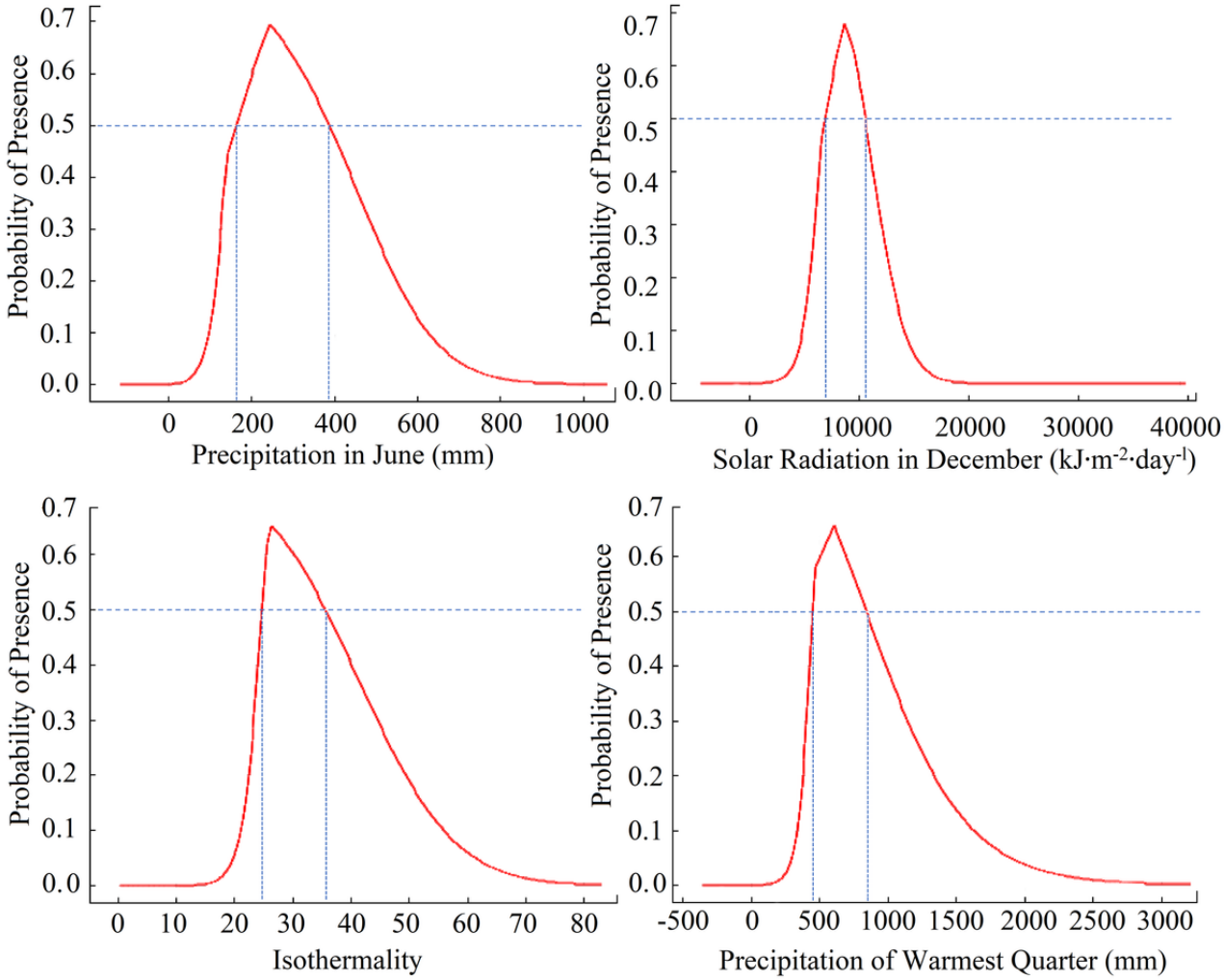

Figure 4

Relationship between existence probability and the dominant environmental factors for *S. javanica.*

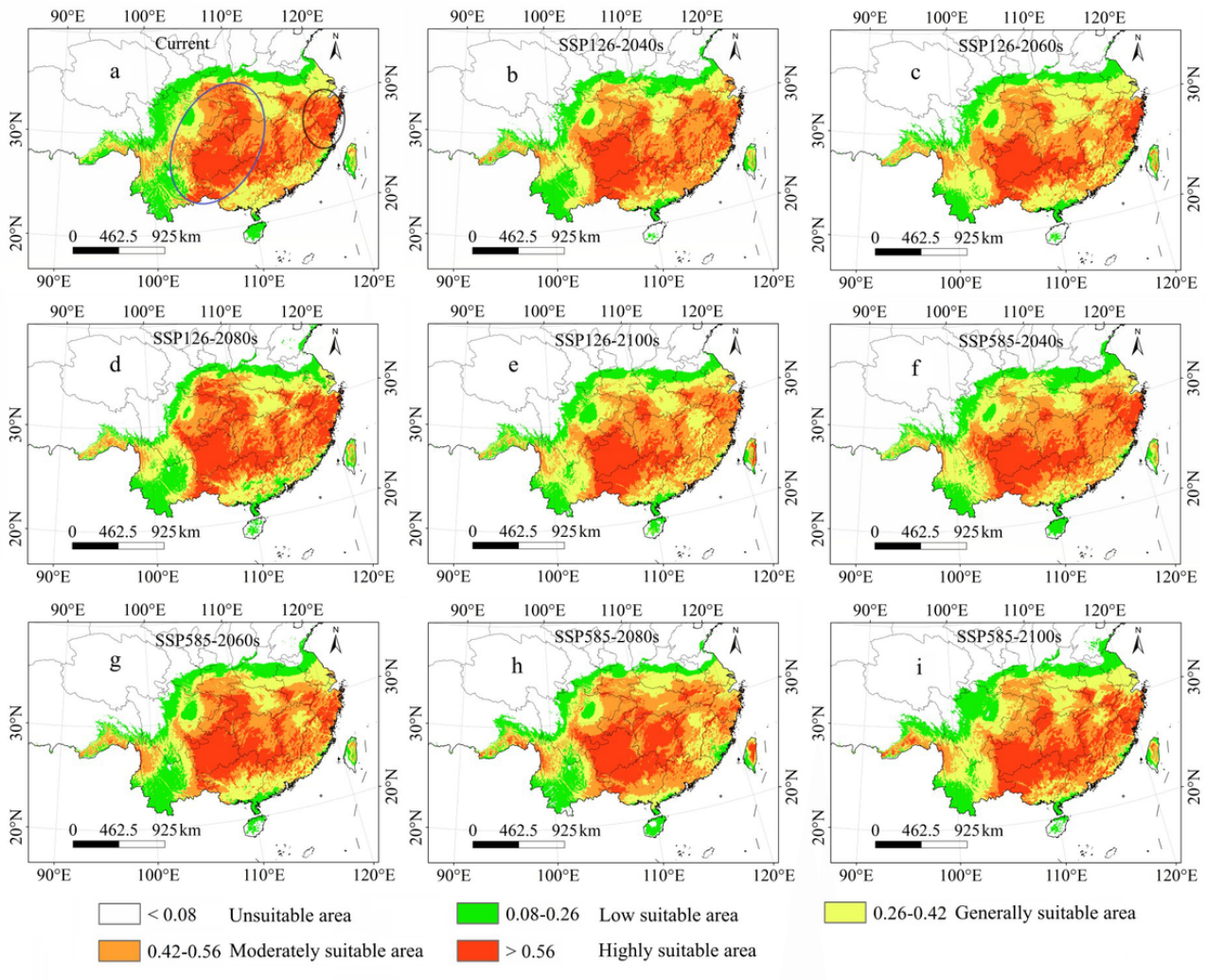

Figure 5

The potential suitable distribution of *S. javanica* in China under different climate scenarios (The blue oval highlights the first suitable distribution region, and the black oval highlights the second suitable distribution regions).

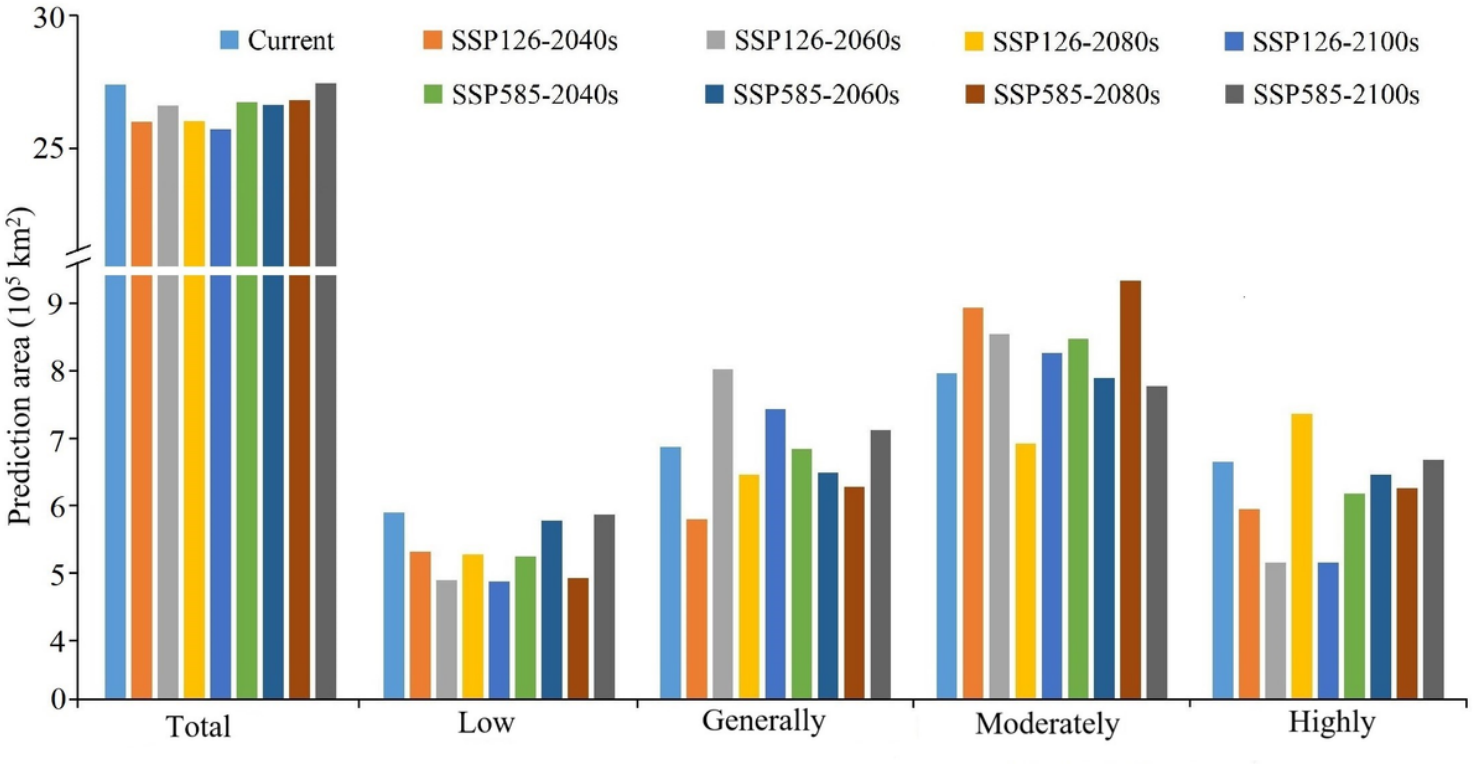

Figure 6

Prediction of the suitable distribution areas of S. javanica under the current and future climate scenarios.